Instrumentation and Measurements for Electron Emission from Charged Insulators

by

Alec M Sim

A thesis proposal submitted in partial fulfillment
of the requirements for the degree

of

MASTER OF SCIENCE

in

Physics

Approved:

Dr. John Robert Dennison Major Professor	Dr. Eric D. Held Committee Member
Dr. Jan J. Sojka Committee Member	Dr. Laurens H. Smith, Jr. Interim Dean of Graduate Studies

UTAH STATE UNIVERSITY
Logan, Utah
February 2005

I. Introduction and Motivation

The electron was first discovered in 1898 by Sir John Joseph Thomson and has since been the subject of detailed study by nearly every scientific discipline. At nearly the same time Heinrich Rudolf Hertz conducted a series of experiments using cathode tubes, high potentials and ultraviolet light. When applying a large potential to a cathode he found that an arching event across the metal plates would occur. In addition, when shining an ultraviolet light on the metal he found that less potential was required to induce the spark. This result, taken together with other electrical phenomena brought about by the shining of light upon metal and was eventually termed the photoelectric effect. The work of Thomson and Hertz represent the beginning of electron emission studies and a body of ideas that pervade nearly all aspects of physics.

In particular these ideas tell us a great deal about the nature of physical interactions within solids. In this thesis we will focus on the emission of electrons induced by an incident electron source over a range of energies, in which one can observe changes in emitted electron flux and energy distribution. In particular, when energetic particles impinge on a solid they can impart their energy, exciting electrons within the material. If this energy is sufficient to overcome surface energy barriers such as the work function, electron affinity or surface charge potential, electrons can escape from the material. The extent of electron emission from the material can be quantified as the ratio of incident particle flux to emitted particle flux, and is termed the electron yield.

The electron yields of materials are relevant to many technical applications:

- Electron multiplier detectors where high-yield materials are desired for more sensitive particle detection[1]
- Scanning electron microscopy where low-energy electron emission provides a means for material surface imaging[2,3]
- Auger electron spectroscopy where core-level electron emission provides a signature of surface elemental composition.
- Plasma fusion devices where low-yield materials are desired such that electron emission does not perturb the surrounding plasma.
- High-current arcing where extensive charge buildup resulting from electron emissions produces electrical arcing either through or across insulators[4]
- Flat panel displays[5] where both high yield emitters and low yield insulators are required.
- Spacecraft charging where NASA's concern results from energetic particle bombardment and electron emissions from spacecraft surfaces in the space environment[6-8]. This in turn can lead to catastrophic systems failure.

The materials characterization facilities at USU have a long and distinguished history[9] of studying electron emission. Although there are many applications in which electron emission is important, the motivation for our studies comes primarily from NASA and its concern for spacecraft charging. Recently, Clint Thomson[9], as a result of his PhD work at USU in spacecraft charging and electron emission from insulating materials, put forth a number of ideas which form the basis for this thesis.

A wide range of theoretical and experimental studies have been conducted to understand spacecraft charging. In particular, to develop a sound understanding of secondary electron emission, the formulation of models based upon an understanding of fundamental physical process in the pre-charge and equilibrium states is required. Recent advances in the knowledge base, technology and theoretical understanding provide an opportunity to contribute significantly to our understanding of the underlying physical mechanisms. In particular, this thesis study will focus on instrumentation upgrades and development that will enhance previous studies and extend our capability. I propose the following instrumentation upgrades:

1. Provide instrumentation to allow for determination of previously unattainable parameters.
2. Decrease data collection and processing time.
3. Improve the quality of data via significant noise reduction.
4. Provide the ability to conduct optical effects studies.
5. Improve sample rotation, alignment and replacement time.

In conjunction with instrumentation upgrades I propose a set of measurements to both verify the new systems operation and provide the measurements of physically interesting mechanisms in insulators. Specifically these measurements will include:

1. Spectra of electron emission and determination of related surface potentials.
2. Total electron emission yields for both neutralized and un-neutralized samples.
3. Alignment characterization for new software and hardware.
4. Characterization of new photo-sources.
5. Characterization of our new flood gun.
6. Implementation of new techniques to understand the time evolution of charging and its effects on electron emission from insulators.

II. Facilities and methods

Utah State University's present materials characterization facility is well suited to electron emission measurements of material properties. At USU electron emission, (EE) studies are performed in an ultra-high vacuum[9] environment for surface contamination control, using an enclosing hemispherical retarding field analyzer and electron, ion, and UV incident sources that allow particle species and energy dependent studies[8,10,11]. The facilities at USU provide state-of-the-art characterization of both conductors and insulators spanning a wide range of applications.

Capabilities for making conductor measurements at USU have been in place for several years[10]. Measurements on conductors utilize a spectrum of beam energies and collection of DC currents from the sample and detector using standard pico ammeters. DC electron emission measurements are stable over long periods of time and therefore are ideal for both measurements of conductors and calibration procedures. In order to make accurate and repeatable measurements standards are essential. Measurements of

conductors are physically easier to interpret and implement than those of insulators. In addition, EE measurements have been performed on conductors for many years[12,13] and are therefore well characterized. The present EE measurement system is calibrated using conductors as standards to measure performance as the system ages and is upgraded. In particular gold and titanium are well characterized both in the literature and at USU and consequently provide good standards.

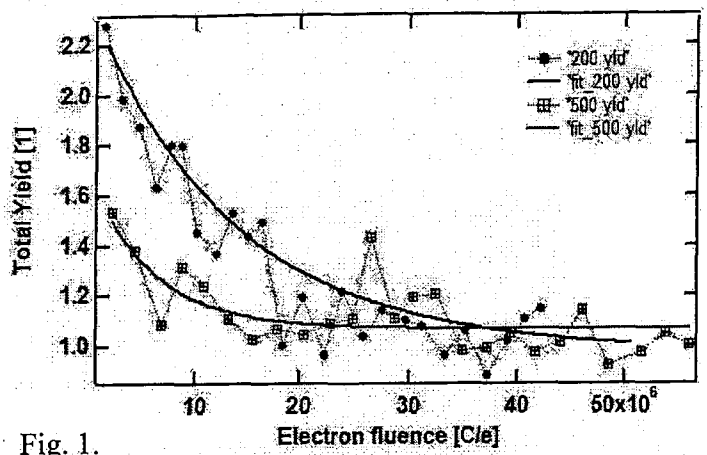

Fig. 1. Change in total yield for two energies 200eV and 500eV. Data taken on Kapton™ with gold backing, here neutralization was used between energies, Alec M Sim 11-2-2004.

Insulators range from relatively simple to complex in material structure and hence are physically more interesting than conductors in many ways. However, measurements of EE from insulators are greatly complicated by the build up of charge within the insulator. For instance, given an electron beam energy E_0 incident on the sample, a net negative charge distribution builds up on or in the sample. This build up of charge occurs quickly for constant electron sources for a wide range of energies. In order to study the material properties of insulators as early in the charging process as possible pulsed-incident electron sources are used.

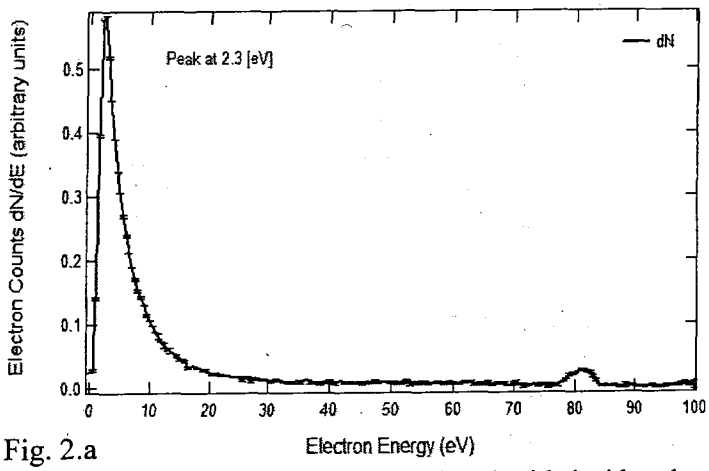

Fig. 2.a Electron emission spectra for Au, induced with incident beam energy of 80eV. Note the peaks as 2.3 and 80eV, respectively. The first results from SE emission and the second is the elastic peak at the beam energy[7]

Recent research at USU[9] has included the development of instrumentation and procedures for measuring the electron-induced emission properties of thick and thin-film insulating materials, using a pulsed-yield technique. This measurement process impinges a small burst of charged particles (typically, ~10^6 electrons per pulse in 5 μs, 30 nA pulses) at a given incident energy on the sample and then measures the EE. However, even at such small fluences, substantial changes have been observed in the insulator yield, (Fig.1), emission spectra, (Fig 2.a, Fig 2.b), and surface charge after only a few

pulses. The resulting sample potentials affect incident electron landing energies, produce energy shifts of the emitted electrons, and consequently lead to significant alterations in the electron emission character[3,14].

To minimize insulator charging, the pulsed-yield process is coupled with a low energy electron neutralization source. The source, a flood gun, uses thermionic emission of low energy electrons near the sample to dissipate positive near-surface charging. However, the neutralization techniques are only effective in a limited range of incident beam energies. For charge distributions created by incident beam currents greater than the second crossover energy, (Sec III) UV discharging must be implemented. These types of studies in which the internal distribution of charge is kept at a minimum are defined as first generation or uncharged studies and are an effective method for determining raw material properties.

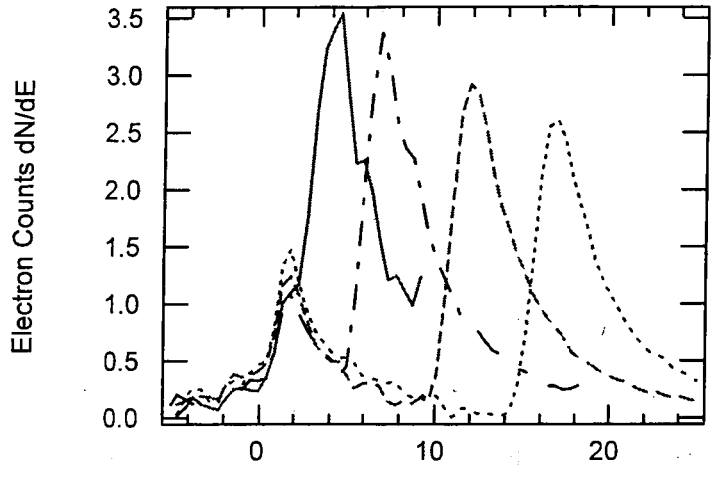

Fig. 2.b Successive plots show secondary electron spectra on negatively biased gold for -2 V (solid), -5 V (dash-dot) and –15V (dot). Successive peaks are measured with respect to the grounded grid peak at (1.8eV). The peak positions correspond to the applied potentials[7], accurate to +/- 1eV.

The present system at USU provides adequate characterization facilities for both conductor and first generation insulator studies. However, previous work at USU by Thomson[9] lends support to the proposed upgrades and experiments. A number of the instrument upgrades proposed in this thesis were suggested by Thomson as a result of his PhD work. The upgrades, (See sec IV) will provide significant improvements in the study of both conductors and insulators. They will allow for both an extension of the current measurements capabilities but also an improvement in the efficiency with which those measurements occur.

III. Electron emission

Electron emission from materials has been studied for over 100 years and provides a well characterized method of study. In general, emitted electrons are separated into two energy regimes defined as secondary and backscattered electrons, SE and BSE respectively. Secondary electrons are defined as those electrons emitted with energy (<50 eV) emitted electrons that originate within the sample, seen as the first peak in (Fig 2.a). Backscattered electrons are typically higher energy electrons (>50 eV) that originate from the incident electron source, but scatter either elastically or inelastically

before leaving the target material. Note that the BSE can contribute to the SE's[15] through scattering within the material. By convention the total yield, σ, is defined as the sum of the SE and BSE. The BSE yield is defined by η and SE yield by δ.

$$\sigma = \delta + \eta \quad (2.0)$$

These parameters are measured as the ratio of respective currents and are defined as follow:

$$\sigma \equiv \frac{I_{SE} + I_{BSE}}{I_{Tot}} \quad (2.1)$$

$$\eta \equiv \frac{I_{BSE}}{I_{Tot}} \quad (2.2)$$

$$\delta \equiv \frac{I_{SE}}{I_{Tot}} \quad (2.3)$$

Where; I_{Tot}, I_{BSE}, and I_{SE} are respectively the total, BSE and SE electron currents to and from the sample. Shown in, (Fig 3) are plots of the total, SE, and BSE yields as a function of incident beam energy for a gold sample.

The total and SE yield curves can be characterized by four points, (Fig 4). These points are the first and second crossover energies E_1 and E_2, the yield peak δ_{max} and the asymptotic limit as the primary beam energy E_0 goes to infinity. The first and second crossover energies occur when the yield is equal to one. Note that for many materials the values of E_1 and E_2 do not exist, as the yield is below one for all energies. In general; for both insulators and metals the crossover energies fall in a range from 20 to 5000 eV[9]. The yield peak is the maximum value that the yield can reach and occurs between the crossover energies. The maximum SE yield is defined as δ_{max} and is generally found in a range of energies E_{max}

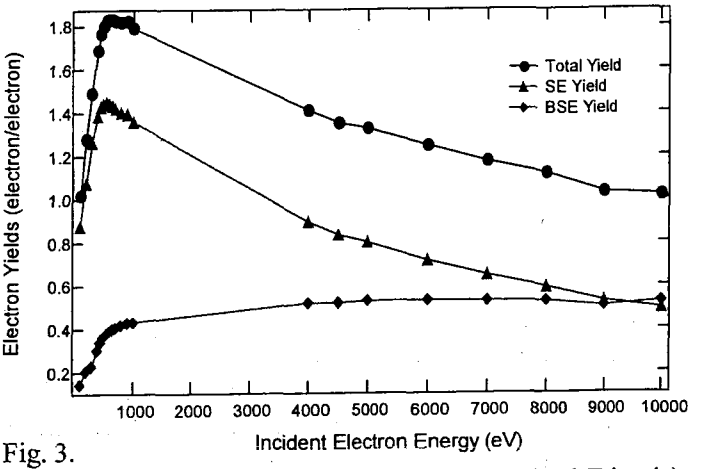

Fig. 3.
Total (Black dot), SE (Blue Triangle), and BSE (Red Triangle) electron yields for Au as a function of incident electron beam energy. Total yield parameters are σ_{max}=1.8±0.1 at E_{max}=600±50 eV. First and second crossover energies[7] (for the total yield) were E_1=100±20 eV and E_2=10000±1000 eV

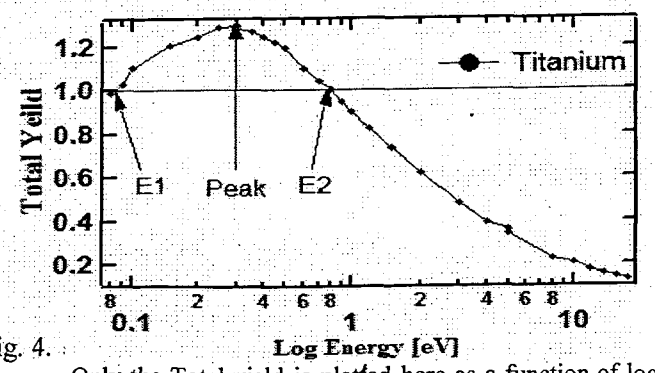

Fig. 4.
Only the Total yield is plotted here as a function of log (energy). Note the arrows to E_1, E_2 and SE max, detailing the general points of interest for such a curve, data taken 10/05/2004 by Alec M Sim.

= (200-1000 eV)[16]. The value δ_{max} is nearly always bounded by the crossover energies, however for materials where E_1 and E_2 do not exits δ_{max} is simply the maximum value reached by the SE yield. In the asymptotic limit of increasing beam energy E_0 the yield goes to zero.

The curve character is, to first, order a result of the relationship between the range R, maximum primary electron penetration depth and λ_{SE}[17] the mean SE inelastic mean free path. In the absences of permanent sample charging one can, to first order, assume that λ_{SE} has a constant mean value. The value R however is dominated by the primary electron beam energy E_0 and varies as approximately a power law $R = C \cdot E_0^n$, where n is empirically determined[9,18]. When the incident beam energy is below E_1, $\lambda_{SE} >> R$ and the SE excitation energy is ($SE_{exitation}$) >> E_0. In this energy range only a dusting of electrons on the surface of the material occurs, leading to a slight negative surface potential. For the energy range $E_1<E_0<E_2$ the value of λ_{SE} is on the order of R. Then, more electrons will be excited to the vacuum interface/surface than are incident and positive surface potentials can result. For E_0 such that $\lambda_{SE} << R$ are electrons less likely to escape. Then, electrons build up creating an internal charge distribution deeper within the sample and therefore a negative surface potential.

Many models have been developed[12,19] to estimate the SE curve. However, few models make good predictions for the curve in all charging regimes and irradiation conditions. In particular, for SE yield curves from insulators, agreement is poor for the high energy tail. The measurements and upgrades proposed in this thesis greatly enhance the possibility of developing a complete understanding of SE through experimentation and our collaborations[10].

IV. Instrumentation and interface upgrades

The present system at USU is adequate for the first generation materials characterization. However, the uncharged or first generation material studies are limited in defining the roles of physical mechanisms that give rise to the EE yield. The improvements proposed in this thesis will provide the opportunity to advance our understanding of the complex mechanisms involved in the secondary electron emission process. In particular, the instrumentation upgrades in this section will provide much improved data collection, instrumentation control and additional measurements not available with the present system. The following outline presents the upgrades and improvements I propose for the computer system and instrumentation. To add detail and motivation to the proposed upgrades both the upgrades and experimental logistics the outline is followed by a subsection review of each item in the outline.

1. Computer system:
    (a) New computer system
    (b) Software development environment
    (c) Data Acquisition Interface Cards, (DAQ)
    (d) General Purpose Interface Bus, (GPIB)
    (e) Present data collection code upgrade
    (f) Electron gun automation

(g) Automation of the sample stage motion

2. Detector housing:
   (a) Inner grid isolation
   (b) Wider beam aperture
   (c) Two LED sources
   (d) Multi-wavelength fiber optic cable
   (e) Low energy flood gun with focusing capabilities
   (f) Faraday cups to enhance the alignment system and beam current monitoring.
   (g) Installation of stage rotation apparatus
   (h) Replacement of relevant feed thorough hardware and wiring upgrade
   (i) Repositioning of key instruments and shortening of wiring

(1) Computer System

(1.a) Computer upgrade

In order to achieve the upgrade of data collection hardware and computer code to a level sufficient for this thesis, the present computer system must be replaced. The present system is a 133 MHz processor with equivalent hardware. This system will be replaced with a 1.5 MHz Dell Optiplex and hardware capable of exceeding the expected demands.

(1.b to 1.e) General improvements in the LabVIEW Code and Computer Control

In the original system[10] National Instruments, (NI) LabVIEW 5.1 was used to develop the software to control GPIB instruments and DAQ Cards. At the time of implementation, a Data Translations DAQ card was used with a legacy GPIB card for the physical interfaces. Since then, there have been significant advances in software and interfacing technology. I propose to implement the following upgrades:

i. NI's LabVIEW 7.1 professional development environment
ii. Two NI 6014 DAQ cards
iii. One NI PCI plug-and-play GPIB interfaces.
   This will significantly increase the sampling rate, (measured in samples per second, SA/s) from 100 SA/s to 50,000 SA/s on each of the DAQ lines and reduce the GPIB talk time significantly.
iv. A number of code upgrades will be implemented including a complete re-coding of the present software. The code development will proceed as follows:
   - First all programs presently in use will be optimized for speed, modular effectiveness and improved user interfacing.

- Second, a system level shell will be implemented that will allow control of all measurement sub routines from a simple user interface.
- Third, an automation management program will be written that allows for decreased user-interface interaction time. This will include the development of :
    - Electron gun control code, (see 1.f)
    - HTML based help system
    - Automated data backup
    - Post process analysis program that will employ Active-X routines and our current analysis program IGOR, allowing for automation of the once lengthy analysis of data

v. In addition, several new sub routines will be written.
- New integration methods for pulsed yield routines
- Peak detection for optimization and signal error tracking
- Material data base manager to allow for simple sample tracking and cut down on repetitive efforts

(1.f) Electron gun and stage (x, y) automation

The automation will remove the user form many aspects of the data collection process and as a result, the data collection time for a typical sample yield will drop by 70%. As a result of the computer system, software and hardware upgrades the data acquisition rate will increase by roughly two orders of magnitude. In addition, the improved processor speed will allow for real time system control and data collection simultaneously. The interfacing and automation of the electron sources are viable. Presently the primary electron beam energies range from 80 to 18000 eV and require two electron guns. For energies in the range of 80 to 5000 eV the Staib gun is used. For energies in the range 5000 eV up to 20,000 eV, a Kimball™ gun is used. The Staib gun is used more often than any other electron gun in the system; we therefore will implement the Staib automation first. The code and consequently the user interface will include the following control options for the Staib gun:

- deflection
- grid
- filament current
- focus
- energy
- standby ramping

In order to interface the Staib gun with the DAQ card a simple 4 bit addressed multiplexed interface will be built that will use a minimum of DAQ outputs in the control of the gun.

(1.g) Automation of the sample stage

In the present system manual alignment is required to position the sample with the electron beam in the x, y plane. An (x, y) rotation control for the sample stage will be installed. This translation system will use a simple stepper motor with sufficient gear reduction. In addition; the control of the rotation will be automated. The capability of the electron gun to optimize on the sample and (x, y, z) translation of the sample stage will provided much improved control over the sample position and beam angle.

(2) Detector housing

(2.a) Electrical isolation the inner grid

Presently, the inner grid, (Fig. 5) is internally tied to ground. Consequently, the DC-spectral method[7] for determining positive sample potentials cannot be used effectively to determine E_1, since the inner grid masks the positive suppression grid potentials required to pull SE's from the positively charged sample surface. The electrical isolation of the inner grid inside the detector housing will allow independent biasing and current monitoring. This alteration will offer a more accurate method for monitoring positive surface potentials using the DC-spectral method. It may also provide the option to improve the energy resolution in spectral measurements by adding another suppression grid to the detector.

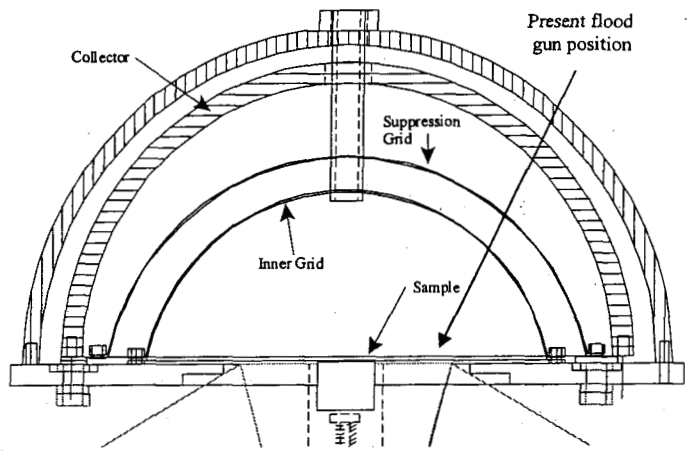

Fig. 5.
Cross-section diagram for present electron emission detector. Note the position of the old flood gun not in figure, where the yellow lines imply the boundary of the sample holder. Here the inner grid is tied to ground.

(2.b) Widen the detector aperture

Optimization of the incident beam onto the sample is critical for accurate electron yield measurements[9]. Conductors can sustain indefinite irritation making them relatively simple to align. For insulators charging occurs very quickly[7]. Instead, alignment for insulators requires that the electron gun and detector aperture are first visually aligned, and then several incident pulses are used to optimize sample and collector currents, causing a pre-charging of the insulator. Widening the aperture to 0.7 cm diameter from 0.5 cm will loosen the tolerances for angular and translational sample stage settings,

making the beam alignment easier. An increased aperture is also critical for alignment of the ion and monochromatic light sources.

(2.c and 2.d) Installation of light sources inside the detector housing

Presently, these studies can only be made by swinging the detector apparatus away from the samples, and then irradiating the samples with lamps through the vacuum chamber port window. This is not only extremely time consuming, but it is very difficult to irradiate the same spot on the sample. Although limited results were seen by Thomson[9], due to the ex-situ nature of the source, levy[20] has reported discharging of deep distributions using a UV source > 4 eV providing support further study. In order to engage in viable studies of photo-discharging the installation of light sources into the detector housing is needed. The following is a list of upgrades and related investigations proposed:

i. Fiber optic for piping in the following sources: (i) monochromatic light from existing quartz, halogen and deuterium discharge sources, (~1200 nm to 180 nm). (ii) New solar simulator source using a filtered Xenon discharge lamp, (~200 nm to 1000 nm). (iii) Other (**infrared**), IR-(**visual**), VIS-(**ultra violet**) UV LED's. (iv) Broadband Deuterium VIS-UV source. (v) Large bore scope to observe and record the sample.

ii. Dual color blue/yellow or green/red LED's

iii. Broadband and monochromatic photo yield measurements and emission spectrum curves.

iv. Broadband and semi-monochromatic flooding to naturalize samples with negative surface charges, particularly as a result of bombardment with $E_0 > E_2$ or $E_0 < E_1$.

(2.e) Mounting the electron flood gun into the detector housing

The electron flood gun presently sits adjacent to the sample in the sample block (Fig 5). This design was originally chosen such that the flood gun could reside inside of the detector apparatus without making further alterations to the detector housing. This design has been both cost effective and relatively easy to implement, but suffers from a few drawbacks. First, the flood gun is powered through the same ribbon cable that carries sample and stage current signals out of the chamber. This monopolizes available sample signal lines and causes signal noise via cross talk. The flood gun will be wired with 22 AWG Kapton-coated wire, rated at 5 A per line and will use a separate UHV feed through. The installation of a single flood gun into the detector housing, pointing towards the sample, (Fig 6) will improve both the gun operation and allow multi-sample testing. Additionally, the implementation of crude focusing capabilities (using an annular electrostatic lens), will allow for low-energy (<80eV) DC-yield measurements assisting in the determination of the first crossover energies of most materials. Presently, the STAIB gun is used to probe E_1, but the minimum operating energy of the gun is ~80 eV such that accurate determination E_1<80 eV is difficult.

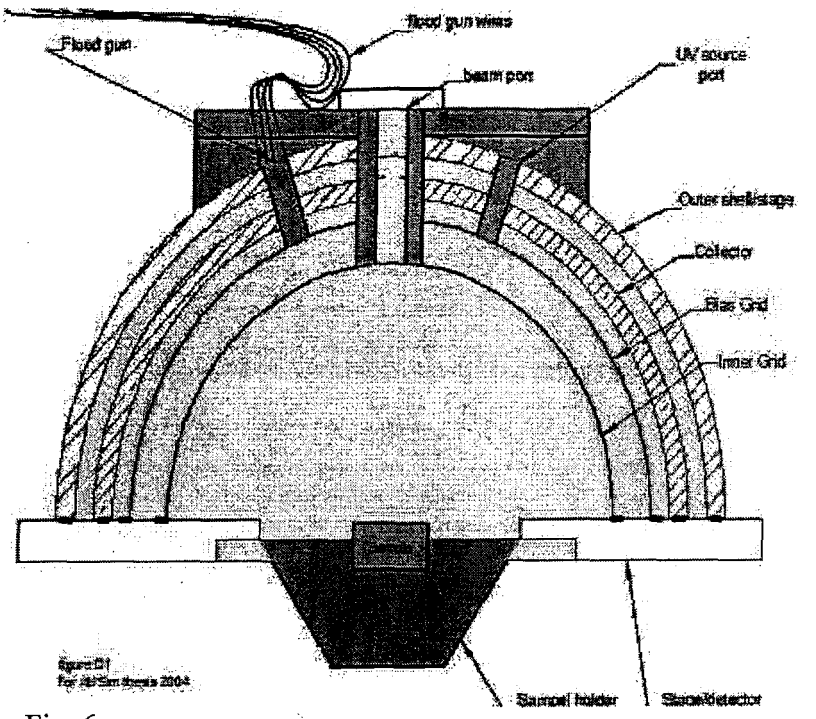

Fig. 6.

Diagram indicated details of proposed detector configuration after upgrades. Note position on new flood gun, UV source and mounting bracket. In addition, the inner grid will be isolated from ground allowing for biasing.

(2.f and 2.g) Faraday cups and alignment system

The implementation of a set of Faraday cups will allow for accurate sample position and beam current to be determined. In the present system, alignment of the sample with an electron gun is done manually. Then, the collector current is optimized using beam deflection controls on a particular electron gun. In order to facilitate automated optimizing a set of small faraday cups will be installed in the exterior of the detector housing, (Fig 6 and Fig 7). The automated system, (see 1.IV) will then use a preset beam deflection sequence to determine both the position of the detector relative to the gun and the position of the beam port. Since the beam port is aligned with the sample the position of the sample will be accurately determined. Then, the software will optimize the beam position on the sample. In addition, another Faraday cup will be installed with a six to one depth to diameter ratio. This will allow accurate determination of the beam current.

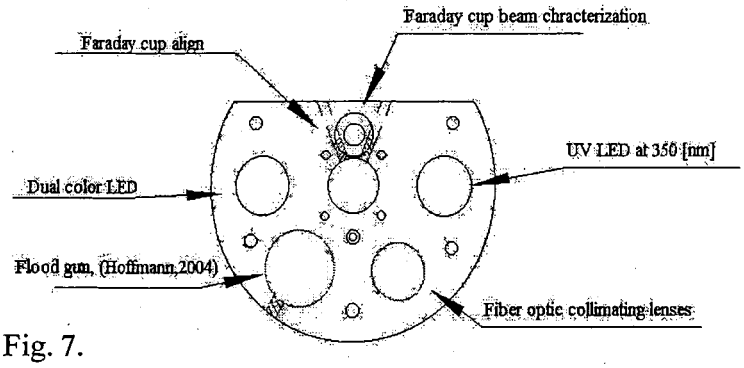

Fig. 7. Top view of proposed detector upgrades. Note that there are four Faraday cups positioned symmetrically about the beam tube that will be used for alignment. In addition there is one six point six to one Faraday cup for beam characterization.

(2.h) Further pulsed system noise reduction

Mounting of instruments closer to UHV wiring outputs[21] will provide both a needed reduction in system noise but also an opportunity to improve the ground plane noise level for the system as a whole. Those instruments include picoammeters, voltage supplies and wiring harnesses. In addition, many of the current coax and triax signal lines will be replaced.

V. Instrumentation validation and experiments

To verify the post upgrade operation and judge the effectiveness of the upgrades a series of previously well characterized measurements will be performed using gold and titanium as standards. This will allow for not only the characterization of the new detector but will provide a test bed for the envisioned software. In particular, the following measurements will be used as verification.

- Electron emission spectra (see Fig. 2.b).

- Total and BSE yields, (Fig. 3 and Fig. 4).
- Automated measurements of the total and BSE yields for DC and pulsed yields.
- Crossover energy determination:
    1. E_2 crossover energy measurements, using the spectral method with higher resolution and accuracy[22].
    2. E_1 determination to test both the isolation of the inner grid and the effectiveness of the spectral method in the low energy range[22].
- Verification of the new optical sources will be done with gold and then insulators. These measurements will include photo-electron yield characterization, for LED's and the fiber optic cable. In addition, we will make preliminary measurements to evaluate the effectiveness of the sources in discharging insulators.
- Test the effectiveness of new sample rotation system.

As a final system verification and lead in to physically interesting data, I propose an investigation of sample current evolution and electron yields as a function of very low levels of incident electron fluences and internal charge accumulation using the pulsed incident electron source, with approximately 10^6 electrons per pulse, (see Fig 1). Also I propose the application of a phenomenological model put forth by Thompson[9] to both fit the new data and highlight physical mechanisms within the material.

In the literature the models presented primarily describe steady-state charging behavior on insulators under continuous electron bombardment[23]. However there are no existing models used to describe the evolving surface potentials, internal charge distributions and electron yields in response to a pulsed incident electron beam prior to reaching the steady state. However there have been simulations and experimental investigations that suggest the constant loss model, presented in Section II is not sufficient to describe SE emission in insulators. A specific example is the work of Kotera and Suga[23] who provided Monte Carlo simulations of incident electron trajectories at E_0=20 [keV], in an insulating material, in response to a pre charge dose, and show that the range R, (see section II) is progressively pushed closer to the surface[9]. In order to facilitate an understanding of the evolution of charge within the material a phenomenological model of dynamic insulator charging has been presented by Thomson[9] that gives a first order estimation of the material decay constant α.

$$\sigma_i = 1 + [\sigma_0 - 1] \cdot \exp\left[-\alpha \cdot \left(\sum_i Q_{0i} \right) \right] \quad (1.0)$$

Equation 1.0 gives the evolving total yield, after i pulses, σ_i as a function of σ_0 the yield of an uncharged insulator prior to irradiation, Q_{i0} the sample charge per pulse and the material decay constant. In particular, simulations by Meyza[9] and measurements by Thomson[9] indicate that the decay constant α of the material, for total yield as a function of incident fluences, is energy dependant. Therefore, a determination of $\alpha(E)$ is needed for a range of energies and materials. In addition, it will be useful to couple this measurement with determinations of the surface potential evolution. Information about the charging rates, internal distribution and charge trapping dynamics within the sample can, in principle, be extracted from the yield as a function of pulse number or fluence[9].

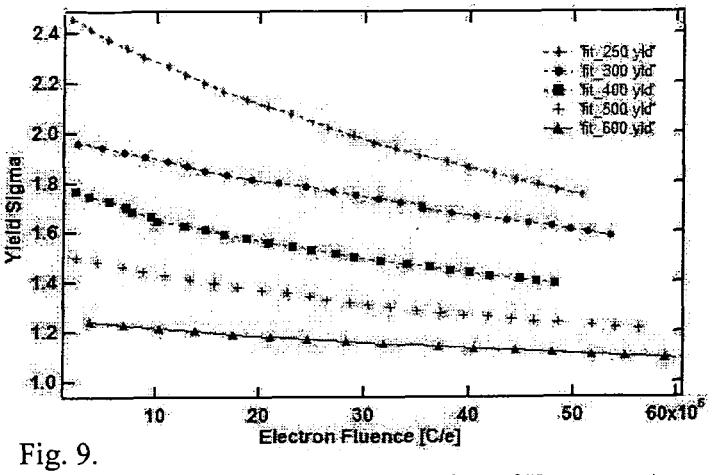

Fig. 9. Exponential fits to yield decay data of Kapton on Au. Note that the Yield decreases with incident energy. Only the fits are shown as the scatter in the data sets presents difficulty in observing individual trends.

As a first step in defining the role of charging dynamics in insulators, I propose a series of measurements and model application, suggested by Thomson[9]. These include the collection of un-neutralized sample yield curves as a function of charge over a spectrum of energies fitted to the phenomenological model, (Fig 9) for Kapton™ and aluminum oxide. Further, the dependence of α on both incident energy and fluence will be studied. In addition, simultaneous spectral measurements to allow accurate determination of the surface potential over a range of energies. In particular, we will look at the energy range between E_1 and E_2, as our system is well calibrated to determine the crossover energies and implement neutralization techniques in this region. Extensions of this study bellow E_1 and beyond E_2 will depend primarily on the effectiveness of the new photo sources in discharging of negatively charged samples. The fitting of Equation 1.0 to these yield curves will provide a determination of α, and subsequently its energy dependence. This data can then be compared to the simulations of Meyza[24] and predictions of Jbara[25] for energy dependence of $\alpha(E)$ and the changing range parameter R(E). In addition, a comparison between decay rates for the charge storage method[26] may provide information about long term space charge decay and the radiation induced conductivity of the sample.

VI. Conclusion

The proposed measurements of conductor and insulator yields, emission spectra, crossover energy determination and decay curves will fully test the extensive proposed system upgrade. The measurements will also validate the enhancements to resolution, range, data acquisition and sample throughput for routine pre-charged measurements of both conductors and insulators. Finally, the proposed study of the incident energy dependence of yield decay curves correlated with sample surface charging should demonstrate one of many possible new types of measurements facilitated by the improvements. Under the best circumstances, significant new physics of charge storage and transport in insulators will be revealed by these new measurements.

Bibliography

1 A. Shih, J. Yater, P. Pehrsson et al., Materials Research Society Symposium Proceedings **416** (Diamond for Electronic Applications), 461 (1996).

2 L. Reimer and M. Riepenhausen, Scanning **7** (5), 221 (1985).

3 H. Seiler, Journal of Applied Physics **54** (11), R1 (1983).

4 M. Belhaj, S. Odof, K. Msellak et al., Journal of Applied Physics **88** (5), 2289 (2000).

5 G. Auday, Ph Guillot, and J. Galy, Journal of Applied Physics **88** (8), 4871 (2000).

6 A. R. Frederickson and J. R. Dennison, IEEE Transactions on Nuclear Science **50** (6, Pt. 1), 2284 (2003).

7 C. D. Thomson, V. Zavyalov, J. R. Dennison et al., NASA Conference Publication 2004-213091 (8th Spacecraft Charging Technology Conference, 2003), 83 (2004).

8 R. E. Davies and J. R. Dennison, Journal of Spacecraft and Rockets **34** (4), 571 (1997).

9 Clint Thomson, Measurements of Secondary Electron Emission properties of Insulators, Dissertation, Utah State University, 2004.

10 Neal Edward Nickles, The role of bandgap in the secondary electron emission of small bandgap semiconductors: studies of graphitic carbon, 2002.

11 Robert Edward Davies, Measurement of angle-resolved secondary electron spectra, 1999; C.D. Thomson; V. Zavyalov; J.R. Dennison; Jodie Corbridge, 8th Spacecraft Charging Conference **1** (2003).

12 Ludwig Reimer, *Scanning Electron Microscopy*. (Springer-Verlag Berlin and Heidelberg GmbH & Co. KG, 1985).

13 E. J. Sternglass, Physical Review **80**, 925 (1950).

14 L. Reimer and H. Drescher, Journal of Physics D: Applied Physics **10** (5), 805 (1977).

15 David C. Joy, Scanning **17** (5), 270 (1995).

16 H. J. Fitting, H. Glaefeke, and W. Wild, Surface Science **75** (2), 267 (1978).

17 L. Reimer, Electron Microsc. Pap. Int. Congr., 10th **1**, 79 (1982).

18 Jacques Cazaux, Journal of Applied Physics **95** (2), 731 (2004); O. Jbara, B. Portron, D. Mouze et al., X-Ray Spectrometry **26** (5), 291 (1997).

19 Ernest J. Sternglass, Physics Review **76**, 189 (1949).

20 L. Levy, D. Sarrail, and J. M. Siguier, 1985.

21 C. D. Thomson, Zavyalov, V., Dennison, J. R., American Physical Society, Annual APS March Meeting 2003, March 3-7, 2003

22 Abbot Jonathan, Methods for Determining Crossover Energies in Insulating Materials (2004).

23 M. Kotera, T. Kishida, and H. Suga, Scanning Microscopy, Supplement **4** (Fundam. Electron Ion Beam Interact. Solids Microsc., Microanal. Microlithogr.), 111 (1990).

24 X. Meyza, D. Goeuriot, C. Guerret-Piecourt et al., Journal of Applied Physics **94** (8), 5384 (2003).

[25] O. Jbara, M. Belhaj, S. Odof et al., Review of Scientific Instruments **72** (3), 1788 (2001).

[26] Prasanna Swaminathan, J. R. Dennison, Alec Sim et al., NASA Conference Publication 2004-213091 (8th Spacecraft Charging Technology Conference, 2003), 157 (2004).